

## The local crystallization in nanoscale diamond-like carbon films during annealing

A. Ya. Kolpakov,<sup>1,a)</sup> A. I. Poplavsky,<sup>1</sup> M. E. Galkina,<sup>1</sup> S. S. Manokhin,<sup>2</sup> and J. V. Gerus<sup>1</sup>

<sup>1</sup>*Problems of Ion-plasma Technologies Development and Implementation Scientific and Research Laboratory, Belgorod State University, 85 Pobeda Str., Belgorod 308015, Russia*

<sup>2</sup>*Nanostructured Materials and Nanotechnologies Science Education and Innovation Centre, 2A Koroleva Street, Belgorod 308034, Russia*

(Received 23 October 2014; accepted 25 November 2014; published online 10 December 2014)

The local crystallization during annealing at 600 °C in nanoscale diamond-like carbon coatings films grown by pulsed vacuum-arc deposition method was observed using modern techniques of high-resolution transmission electron microscopy. The crystallites formed by annealing have a face-centred cubic crystal structure and grow in the direction  $[0\bar{1}\bar{1}]$  as a normal to the film surface. The number and size of the crystallites depend on the initial values of the intrinsic stresses before annealing, which in turn depend on the conditions of film growth. The sizes of crystallites are 10 nm for films with initial compressive stresses of 3 GPa and 17 nm for films with initial compressive stresses of 12 GPa. Areas of local crystallization arising during annealing have a structure different from the graphite. Additionally, the investigation results of the structure of nanoscale diamond-like carbon coatings films using Raman spectroscopy method are presented, which are consistent with the transmission electron microscopy research results.

[<http://dx.doi.org/10.1063/1.4903803>]

The negative influence of high intrinsic compressive stresses in diamond-like carbon (DLC) films with a high content of  $sp^3$ -phase, restraining their widespread application in micromechanics, is well known.<sup>1,2</sup> However, many researchers use the intrinsic stresses purposefully to form carbon coatings with special properties. In particular, the investigation of multilayer carbon-based structures, with different contents of  $sp^3$  and  $sp^2$ -phases, which are characterized by different values of electrical conductivity and the internal stresses, is described.<sup>3,4</sup> In this case, the changing accelerating potential of the substrate is used. It allows to accelerate carbon ions and forms layers with different properties, which is necessary for the method of vacuum-arc deposition with the filtration of the plasma flow.<sup>5</sup>

The structure and electrical properties of the tetrahedral amorphous carbon (ta-C) films with 70%–88%  $sp^3$  content were investigated by atomic force microscopy (AFM), transmission electron microscopy (TEM), and Raman spectroscopy as a function of annealing temperature in the range of 25–1100 °C.<sup>6</sup> TEM investigation is confirmed that the clusters appear not only at the surface of the films but also in the bulk. The growth and the partial orientation of the  $sp^2$ -bonded nanoclusters in the size range of 1–3 nm are accompanied by a large reduction in the film intrinsic stress, which decreases sharply in the temperature range of 500–600 °C. Therefore, temperature of 600 °C was selected in the present work as the critical temperature at which significant changes in the structure and properties of carbon coatings are beginning.

The pulsed vacuum-arc method<sup>7</sup> for deposition of DLC films allows to exclude the using of the electrostatic ion acceleration by applying a negative potential to the substrate

and to reduce undesirable heating of the carbon film during the deposition, which lead to its graphitization. The flow of carbon plasma generated by a pulsed source of carbon plasma with ions energy of 40–100 eV can be oriented in a desired direction with respect to the substrate and thus the value of internal stresses can be changed from 12 GPa to 3 GPa.<sup>8</sup>

The present work deals with the structural changes and changes in the intrinsic stresses that occur when pulsed vacuum arc grown DLC films are annealed at 600 °C in vacuum. Our study is focused on the effect of initial values of the intrinsic stresses on the structure of DLC films during annealing. The films were obtained at different orientations of the substrate with respect to the flow of carbon plasma. To monitor the current changes, we use modern techniques of transmission electron microscopy, in particular, high-resolution TEM (HRTEM) and electron energy-loss spectroscopy (EELS),<sup>9</sup> as well as Raman spectroscopy.<sup>10</sup> Our investigation aims to expand the understanding of the stress relaxation mechanisms during annealing and relate them to the structural changes that occur in nanosized carbon DLC films grown by pulsed vacuum-arc method.

The samples for investigation were obtained by pulsed vacuum-arc deposition method using a UVNIPA-1-001 unit equipped with a pulsed source of carbon plasma with a consumable graphite cathode made of MPG-6 graphite. Prior to the deposition, the substrate was subjected to ion cleaning using ion source type II-4-0.15. The films of 70–100-nm thickness were deposited on polished monocrystalline silicon plates and on freshly cleaved monocrystal NaCl. Two types of test samples of carbon coatings were investigated: obtained at horizontal orientation of the substrate with respect to carbon plasma flow (DLC-I) and obtained at vertical orientation of the substrate (DLC-II), illustrated in Figs. 1(a) and 1(b), respectively.

<sup>a)</sup> Author to whom correspondence should be addressed. Electronic mail: [kolpakov@bsu.edu.ru](mailto:kolpakov@bsu.edu.ru)

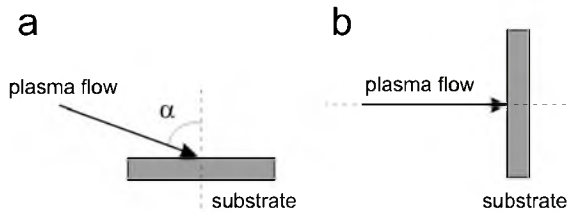


FIG. 1. Scheme for obtaining the test samples of carbon coatings: (a) DLC-I and (b) DLC-II.

Carbon coatings were separated from the NaCl substrate in distilled water and placed on a copper grid. Then, one of the samples on the copper grid was placed in a vacuum furnace GHA 10/600 made by "Carbolite" company and annealed at 600 °C for 10 min. The heating time was 40 min. The annealed samples were removed from the furnace on the next day after its complete cooling.

The value of the internal stress was determined before and after annealing by laser-optical method.<sup>11</sup>

Considering the complexity of the characterization of DLC coatings with disordered structure, we used for the investigation the capabilities of HRTEM. Electron energy loss spectra, as well as the plasmon energy, were obtained by EELS using Tecnai G2 F20 transmission electron microscope equipped with a 860 Gatan Imaging Filter (GIF) 2001. To calculate the average particle size, the histograms of particle size distribution for horizontal and vertical secants were used for the both samples. Then using these histograms, the averaged histogram was constructed. The mean particle size was evaluated from the averaged diagram. Raman spectra were obtained on Renishaw inVia Basis spectrometer, and the wavelength of the laser was 514 nm.

According to the investigation results obtained by TEM, the structure of DLC-I and DLC-II in as-deposited state is amorphous and almost homogeneous. The internal compressive stresses in as-deposited state are equal to 3 GPa in DLC-I and 12 GPa in DLC-II.

Figs. 2(a) and 2(b) show dark field TEM images of the investigated films after annealing at 600 °C in a vacuum. The values of the internal stresses in the both specimens after their annealing are equal to 2 GPa.

There is a dramatic difference between the structure of the samples in as-deposited state and after annealing. Fig. 2 shows the local light areas with size of about 10–20 nm in

the structure of the films after annealing. Moreover, comparing the structure of the films after annealing in Figs. 2(a) and 2(b), one can conclude that the number and size of the local light areas depend on the initial orientation of the substrate during the deposition of the coating or the initial values of compressive stresses. In particular, there is a greater number of local light areas in DLC-II (Fig. 2(b)) compared with DLC-I (Fig. 2(a)). In addition, in Fig. 2(b), the greater scatter in the size of local light areas is observed.

To calculate the size of the local light areas, the method of secants was used. This method takes into account all possible variants of the cross sections of the particles and the average value is determined based on a large sample (for vertical and horizontal secants). The average size of these areas is  $10 \pm 2$  nm for DLC-I and  $17 \pm 1$  nm for DLC-II.

In order to perform a detailed analysis of the local light areas, HRTEM investigation was carried out. HRTEM-images of local light areas in the structure of the annealed samples are shown on Fig. 3. HRTEM images (Fig. 3) show the particular cases of the separate light particles that are nanocrystallites with sizes of  $6.12 \times 7.77$  nm and  $13.33 \times 19.14$  nm. Probably, light particles in DLC-II may consist of several crystallites with high angle boundaries (boundaries with misorientation angle of more than 15°) (Fig. 3(b)). On the other hand, this figure does not exclude that the crystallites have formed conglomerate consisting of separate nanocrystals. It is worth mentioning that these features were not considered at the calculation of the average size of the light particles, and the size of the whole particle rather than its separate components was determined. The light particles were not observed in the structure of the samples in the initial state (before annealing).

It was found that these areas correspond to the nanoscale crystallites with face-centred cubic (FCC) structure. Furthermore, it was defined that the interplane spacings are 2.47 Å ( $\bar{1}\bar{1}1$ ), 2.13 Å (200), and 1.51 Å (022) for the both samples. The calculated lattice parameter for the FCC phase is  $4.27 \pm 0.01$  Å and the unit cell volume is  $0.78 \text{ \AA}^3$  (the unit cell volume of the diamond is  $0.45 \text{ \AA}^3$ ). There are number of different modifications of carbon, including modifications with the cubic lattice.<sup>12</sup> According to Refs. 13–15, lattice parameter  $a$  may be in the range from 3.33 to 5.2 Å. Numerous carbon modifications were found by chemical vapor deposition (CVD) of thin films.<sup>16,17</sup> In most of the studies, the lattice constant assumes the value of  $3.6 \pm 0.05$  Å.

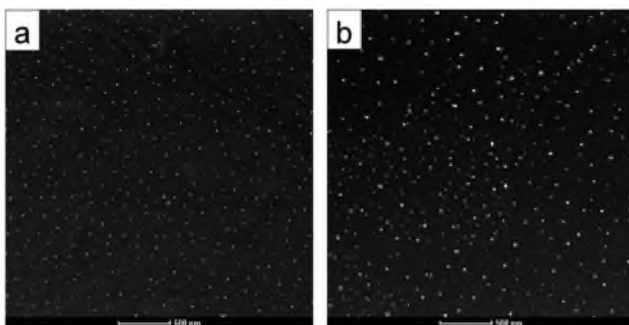


FIG. 2. Dark field TEM images of carbon film after annealing in vacuum at 600 °C: (a) DLC-I and (b) DLC-II.

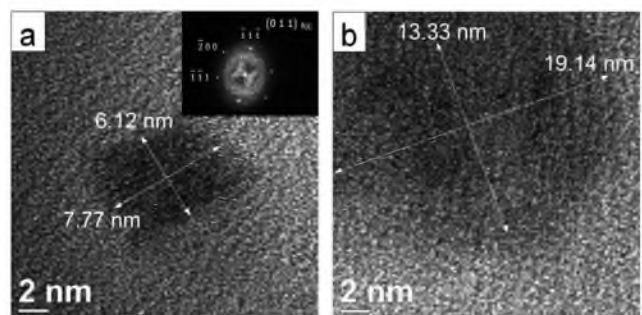


FIG. 3. HRTEM image of light area in the structure of carbon films after annealing at 600 °C in vacuum: (a) DLC-I and (b) DLC-II.

Furthermore, it should be noted from the HRTEM-images that the crystallites form with the [011] direction of FCC lattice, normally to the film surface. Another feature of ordered regions developed during annealing is that they are composed of several crystallites in the DLC-II (shown by arrows in Fig. 3(b)).

The plasmon energy in as-deposited state is approximately 29 and 30 eV for the DLC-I and DLC-II, respectively. The plasmon energy for the areas with an ordered structure is about 30 eV for the both annealed samples.

Raman spectroscopy is a generally accepted method of characterization of crystalline, nanocrystalline, and amorphous carbon structures, thus our study was supplemented by the research results of Raman spectra (Figs. 4 and 5). In order to define the position of the G and D peaks, we presented the experimental spectra as a sum of two Gaussian curves. Structural changes in the carbon coating during annealing will be associated with the position of G-peak and integrated intensity ratio  $I(D)/I(G)$ .

Fig. 4 shows the Raman spectra of DLC-I before and after annealing. The position of G-peak before annealing corresponds to  $1563\text{ cm}^{-1}$  and  $I(D)/I(G) = 0.46$ . After annealing at  $600\text{ }^{\circ}\text{C}$ , G-peak increases to  $1578\text{ cm}^{-1}$  and  $I(D)/I(G)$  increases to 0.77.

Raman spectra of DLC-II before and after annealing represent a slightly asymmetric peak without apparent separation of the D- and G-peaks (Fig. 5). G-peak position before annealing corresponds to  $1572\text{ cm}^{-1}$ , and  $I(D)/I(G) = 0.17$ . Annealing at  $600\text{ }^{\circ}\text{C}$  does not lead to appreciable changes in the Raman spectrum, and the position of G-peak corresponds to  $1570\text{ cm}^{-1}$  and  $I(D)/I(G) = 0.18$ . Such spectra are typical for ta-C films with a low content of  $\text{sp}^2$ -phase.

The shift of the G-peak toward higher frequencies with simultaneous increasing of the  $I(D)/I(G)$  ratio is the common feature of the transition from ta-C carbon to nanocrystalline graphite and is caused by the following processes: (1) the conversion of some carbon atoms from the  $\text{sp}^3$ - to  $\text{sp}^2$ -hybridization; and (2) the clustering of atoms with  $\text{sp}^2$ -

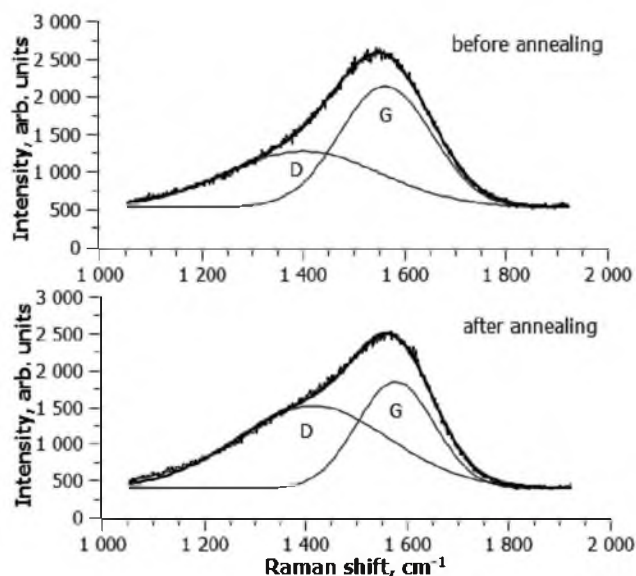


FIG. 4. Raman spectra of DLC-I before and after annealing.

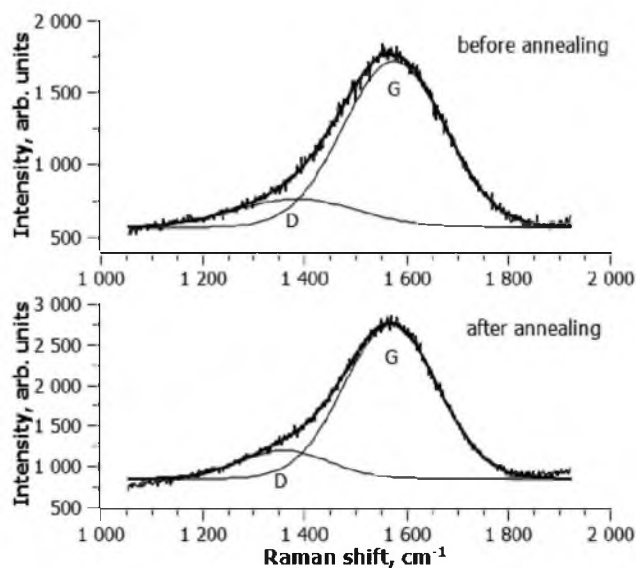


FIG. 5. Raman spectra of DLC-II before and after annealing.

hybridization with the formation of ordered structures.<sup>10</sup> Comparing the results of Raman spectroscopy and HRTEM, one can conclude that the areas of the local crystallization have a structure different from graphite, since an increase in the number and size of the nanocrystallites does not lead to appreciable changes in the Raman spectra of DLC-II. Thus, it can be argued that the DLC-II with a high content of  $\text{sp}^3$ -phase has a higher thermal stability.

Our previous studies have shown that annealing of carbon coatings at  $600\text{ }^{\circ}\text{C}$  leads to an increase in wear resistance.<sup>18</sup> Currently, we have obtained preliminary experimental results showing an increase of microhardness carbon coatings after a similar heat treatment; however, the role of local crystallization in this process remains to be seen.

In summary, the effect of the vacuum annealing at  $600\text{ }^{\circ}\text{C}$  on the structure of the diamond-like carbon films deposited by pulsed vacuum-arc method has been examined in this paper. High-resolution transmission electron microscopy investigation directly shows that annealing leads to local crystallization (ordering) of the film structure and the formation of nanocrystallites. The number and size of the crystallites depend on the initial values of the intrinsic stresses before annealing, which in turn depend on the conditions of film growth. The size of crystallites is  $10 \pm 2\text{ nm}$  for films with initial compressive stresses of 3 GPa and is  $17 \pm 1\text{ nm}$  for films with initial compressive stresses of 12 GPa. The crystallites formed in the films with intrinsic stresses of 12 GPa after annealing are polycrystalline. The crystallites have a face-centred cubic structure and grow with  $[011]_{\text{FCC}}$  as a normal to the film surface during annealing. Interplanar spacings in the crystallites irrespective of the value of initial intrinsic stresses are equal to  $d = 2.47\text{ \AA}$  ( $\bar{1}\bar{1}1$ )<sub>FCC</sub>,  $d = 2.13\text{ \AA}$  (200)<sub>FCC</sub>, and  $d = 1.51\text{ \AA}$  (022)<sub>FCC</sub>. The results of electron energy-loss spectroscopy analysis demonstrate that the value of the plasmon energy of 29–30 eV slightly increased to about 30 eV during annealing. Comparison of the Raman spectroscopy and transmission electron microscopy research results leads to the conclusion that the areas of local crystallization arising during annealing have a structure different from the graphite.

The authors are grateful to Dr. A. N. Belyakov for assistance in preparing this article for publication.

- <sup>1</sup>J. M. Jungk, B. L. Boyce, T. E. Buchheit, T. A. Friedmann, D. Yang, and W. W. Gerberich, *Acta Mater.* **54**, 4043 (2006).
- <sup>2</sup>S. Weissmantel, G. Reisse, and D. Rost, *Surf. Coat. Technol.* **188–189**, 268 (2004).
- <sup>3</sup>D. G. McCulloch, X. L. Xiao, J. L. Peng, P. C. T. Ha, D. R. McKenzie, M. M. Bilek, S. P. Lau, D. Sheeja, and B. K. Tay, *Surf. Coat. Technol.* **198**, 217 (2005).
- <sup>4</sup>D. W. M. Lau, D. G. McCulloch, M. B. Taylor, and J. G. Partridge, *Phys. Rev. Lett.* **100**(1), 176101 (2008).
- <sup>5</sup>R. L. Boxman, V. Zhitomirsky, B. Alterkop, E. Gidalevich, I. Beilis, M. Keidar, and S. Goldsmith, *Surf. Coat. Technol.* **86–87**, 243 (1996).
- <sup>6</sup>J. O. Orwa, I. Andrienko, J. L. Peng, and S. Praver, *J. Appl. Phys.* **96**(11), 6286 (2004).
- <sup>7</sup>A. I. Maslov, G. K. Dmitriev, and Y. D. Chistyakov, *Prib. Tekh. Eksp.* **3**, 146 (1985).
- <sup>8</sup>A. Ya. Kolpakov, V. N. Inkin, and S. I. Ukhanov, RF Patent No. 2240376 C1 (2004).
- <sup>9</sup>R. F. Egerton, *Rep. Prog. Phys.* **72**, 016502 (2009).
- <sup>10</sup>A. C. Ferrari and J. Robertson, *Phys. Rev. B* **61**(20), 14095 (2000).
- <sup>11</sup>A. Ya. Kolpakov, A. I. Poplavsky, M. E. Galkina, I. V. Sudzhanskaya, and O. Yu. Merchansky, *Uprochnyayushie tehnologii I pokrytiya* **4**(88), 40 (2012).
- <sup>12</sup>L. S. Palatnik, M. B. Guseva, V. G. Babaev, N. F. Savchenko, and I. I. Fal'ko, *Sov. Phys. JETP* **60**, 520 (1984).
- <sup>13</sup>S. Aisenberg and R. Chabot, *J. Appl. Phys.* **42**, 2953 (1971).
- <sup>14</sup>E. G. Spencer, P. H. Schmidt, D. C. Joy, and F. J. Sansalone, *Appl. Phys. Lett.* **29**, 118 (1976).
- <sup>15</sup>M. Sokolowski, A. Sokolowska, B. Gokieli, A. Michalski, A. Rusek, and Z. Romanowski, *J. Cryst. Growth* **47**, 421 (1979).
- <sup>16</sup>S. Jarkov, Y. Titarenko, and G. Churilov, *Carbon* **36**(5–6), 595 (1998).
- <sup>17</sup>N. F. Savchenko, M. B. Guseva, V. V. Khvostov, Yu. A. Korobov, and V. G. Babaev, *Nanosistemy. Nanomaterialy. Nanotekhnologii* **8**(2), 455 (2010).
- <sup>18</sup>M. G. Kovaleva, A. J. Kolpakov, A. I. Poplavsky, and M. E. Galkina, *J. Frict. Wear* **34**(6), 481 (2013).